# Topological molecules and topological localization of a Rydberg electron on a classical orbit

Ali Emami Kopaei,[1,*] Xuedong Tian,[1,2,*] Krzysztof Giergiel,[1,3] and Krzysztof Sacha [1]

[1]*Instytut Fizyki Teoretycznej, Uniwersytet Jagielloński, ulica Profesora Stanisława Łojasiewicza 11, PL-30-348 Kraków, Poland*
[2]*College of Physics Science and Technology, Guangxi Normal University, 541004 Guilin, China*
[3]*Optical Sciences Centre, Swinburne University of Technology - Hawthorn, Victoria 3122, Australia*

It is common knowledge that atoms can form molecules if they attract each other. Here, we show that it is possible to create molecules where bound states of the atoms are not the result of attractive interactions but have the topological origin. That is, the bound states of the atoms correspond to the topologically protected edge states of a topological model. Such topological molecules can be realized if the interaction strength between ultracold atoms is properly modulated in time. A similar mechanism allows one to realize topologically protected localization of an electron on a classical orbit if a Rydberg atom is perturbed by a properly modulated microwave field.

*Introduction*. Experiments often suffer from imperfections and external perturbations that are difficult to eliminate. The situation can change if the state which has to be realized in the laboratory is protected by topology. The phenomena determined by topological invariants are robust unless a perturbation is so strong that it changes the topology. For example, we may dramatically deform a torus, but it is still the same topological object unless we cut it. The range of topologically protected phenomena is broad, from the quantum Hall effect to ideas of topological quantum computation [1,2].

In this Letter, we address the question of whether bound states of atoms or localization of a Rydberg electron on a classical orbit can be protected by topology. It would be vital to experimentalists because these objects would be robust and resistant to external perturbations. To accomplish our objectives, we employ *time engineering* developed in the field of time crystals and phase space crystals, which allows the realization of condensed matter physics in the time domain [3–5] (for reviews, see [6–9]). Basically it relies on resonant periodic perturbation of, e.g., ultracold atoms, which effectively behave like a solid-state system.

*Localization of a Rydberg electron.* Let us begin with a highly excited hydrogen atom. Even if the electron is highly excited and prepared in a localized wavepacket, the classical picture of a particle moving on a Kepler orbit is quickly lost due to the spreading of the wavepacket over the entire classical orbit [10]. Spreading can be suppressed if the atom is driven resonantly by an electromagnetic field [10–12]. Then, in the frame moving along a Kepler orbit, a potential well is created that supports the wavepacket, and the classical picture of the electron circulating around the nucleus can be experimentally demonstrated [13–16]. There is also an idea to prevent

the electron from spreading by employing a fluctuating microwave field [17]. That is, a fluctuating microwave field induces destructive interference phenomena that are responsible for Anderson localization of an electronic wavepacket on a classical orbit. Signatures of Anderson localization of a Rydberg electron can also be observed if ground-state atoms are immersed within a Rydberg wavefunction [18].

To show that the electron in a hydrogen atom can be represented by a wavepacket whose localization is protected by topology, let us consider a H atom in the presence of a static electric field and two linearly polarized microwave fields with frequencies $\omega$ and $2\omega$ and a certain superposition of their subharmonics and harmonics $f(t) = f(t + s2\pi/\omega) = \sum_{k \neq 0} f_k e^{ik\omega t/s}$ where $s$ is integer. The Hamiltonian of the system in the atomic units reads

$$H = \frac{\mathbf{p}^2}{2} - \frac{1}{r} + z[F + F_1 \cos(\omega t) + F_2 \cos(2\omega t) + \lambda f(t)], \tag{1}$$

where $F$, $F_j$, and $\lambda$ are the strength of the electric field and the amplitudes of the microwave fields, respectively. Before we present quantum results, we derive a classical effective Hamiltonian that allows us to understand how the phenomenon, in which we are interested, emerges.

The natural variables for the classical description of a H atom are the action angle variables, where $I$ is the principal action (the classical analog of the principal quantum number $n$), $L$ is the total angular momentum, and $\theta$ and $\psi$ are the corresponding conjugate canonical variables that describe the position of the electron in a Kepler orbit and the angle between the major axis of the elliptical orbit and the $z$ axis, respectively [10]. We assume that the projection of the angular momentum of the electron on the $z$ axis, which is a constant of motion, is zero. We also assume that the microwaves are resonant with unperturbed electronic motion, i.e., the ratio of the frequency $\omega$ and the frequency of the electronic motion is an integer number $s = \omega I_s^3$ where $I_s$ is the resonant value

*These authors contributed equally to this work.

of the principal action [$s$ is the same as in the expression of $f(t)$]. In the frame moving along the orbit, $\Theta = \theta - \omega t/s$, all dynamical variables are slowly varying if we are close to the resonant trajectory, i.e., if $P = I - I_s \approx 0$. By averaging the Hamiltonian over time $t$, we obtain the effective (secular) Hamiltonian [19,20],

$$H_{\text{eff}} = \frac{P^2}{2m_{\text{eff}}} + V_1 \cos(s\Theta) + V_2 \cos(2s\Theta) + \lambda V_b(\Theta), \quad (2)$$

where a constant term is omitted, the effective mass $m_{\text{eff}} = -I_s^4/3$, $V_1 = -I_s^2 F_1 \mathcal{J}_s'(s)/s$, $V_2 = -I_s^2 F_2 \mathcal{J}_{2s}'(2s)/2s$, and $V_b(\Theta) = -I_s^2 \sum_{k \neq 0} f_{-k} \mathcal{J}_k'(k) e^{ik\Theta}/k$, where $\mathcal{J}_k'$'s are derivatives of the ordinary Bessel functions. The effective Hamiltonian (2) describes the motion of the electron around the elongated Kepler ellipse with the total angular momentum $L = 0$. This orbit is aligned along the $z$ axis ($\psi = 0$) and is stable, provided that the static electric field is sufficiently strong [20,21].

If $\lambda = 0$ and $s \gg 1$, the Hamiltonian (2) shows that the electron in a H atom, in the frame moving along the elongated resonant orbit, behaves the same way as an electron in a crystalline structure with a two-point basis. Actually, if we quantize the classical Hamiltonian (2) and restrict ourselves to its first two energy bands, we arrive at the Su-Schrieffer-Heeger model [22], which is topologically nontrivial if $V_1/V_2 > 0$, i.e., it is characterized by the nonzero winding number [23,24]. This is a simple model of a topological insulator that has been investigated theoretically and experimentally in many different systems [23,25–28]. A striking property of topological insulators with edges is the presence of topologically protected states that are localized at the edges [23]. To introduce an edge in the potential in (2), we turn on the subharmonics and harmonics of the microwave field ($\lambda \neq 0$) prepared so that the additional potential $\lambda V_b(\Theta)$ describes a barrier located at a certain $\Theta$. Then, the spectrum of the quantized version of $H_{\text{eff}}$ reveals a pair of energy levels in the gap between two bands and the corresponding eigenstates are localized close to the edge (see Fig. 1).

So far we have described a H atom by means of the classical effective Hamiltonian which at the end is quantized. However, the entire description can be performed fully quantum mechanically starting with (1). When we switch to the moving frame by means of the unitary transformation $e^{i\hat{n}\omega t/s}$, where $\hat{n}$ is the principal quantum number operator, and average the Hamiltonian over $t$, we obtain the matrix of the quantum effective Hamiltonian

$$\langle n', l' | \hat{H}_{\text{eff}} | n, l \rangle = \left( -\frac{1}{2n^2} - n\frac{\omega}{s} \right) \delta_{nn'} \delta_{ll'} + \langle n', l' | z | n, l \rangle$$
$$\times [F\delta_{nn'} + F_1(\delta_{n+s,n'} + \delta_{n-s,n'})/2$$
$$+ F_2(\delta_{n+2s,n'} + \delta_{n-2s,n'})/2 + \lambda f_{n-n'}], \quad (3)$$

where $|n, l\rangle$ is a hydrogenic eigenstate with the principal quantum number $n$, total angular momentum $l$, and the projection of the angular momentum on the $z$ axis equal to zero. The spectra of the quantized classical Hamiltonian (2) and the quantum Hamiltonian (3) are compared in Fig. 1. In Fig. 2 we present the time evolution, in the laboratory frame, of an eigenstate of (3) corresponding to one of the edge states identified with the help of the Hamiltonian (2). One can see that
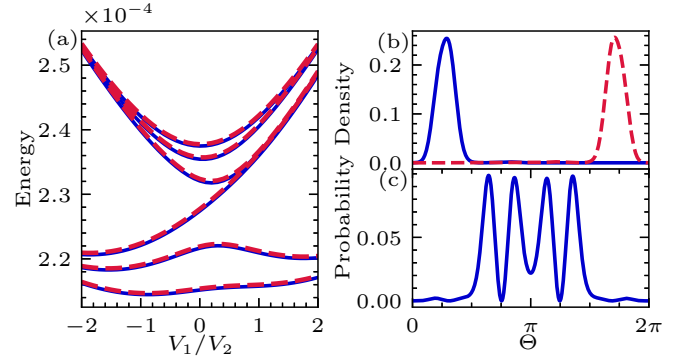


FIG. 1. Topological localization of a Rydberg electron. Panel (a) shows the spectrum of the quantized version of the classical Hamiltonian (2) (red dashed lines) and the corresponding energy levels of the quantum effective Hamiltonian (3) (solid blue lines) for $s = 4$. For $V_1/V_2 > 0$, two edge states of the Hamiltonian (2) form with nearly degenerate energies visible in the middle of the spectrum. Energy values are presented in the atomic units multiplied by $n_s^2$ and the constant term $-3/2$ is subtracted. Panel (b) presents probability densities of these two edge states for $V_1/V_2 = 2$—the edge is located around $\Theta = 0$ (or equivalently $\Theta = 2\pi$) and the edge states localize close to it. Other eigenstates (bulk states) are delocalized along the entire range of $\Theta$ [in (c) the fifth excited eigenstate of (2) is shown]. The parameters of the system are the following: the resonant principal quantum number $n_s = I_s = 800$, $n_s^3\omega = 4$, $n_s^4 F = 1.5 \times 10^{-4}$, $n_s^4 F_1 = 1.258 \times 10^{-3}$, $n_s^4 \lambda = 1.172 \times 10^{-5}$, and $f_k = e^{ik\epsilon} \cos(k\pi/21) \text{sinc}^2(k\pi/14) k/J_k'(k)$ with $\epsilon = 5 \times 10^{-3}$ for $|k| \leqslant 20$ and $f_k = 0$ for higher $|k|$ [29]. In (b) and (c), $n_s^4 F_2 = 1.93 \times 10^{-3}$. Quantities are in atomic units.
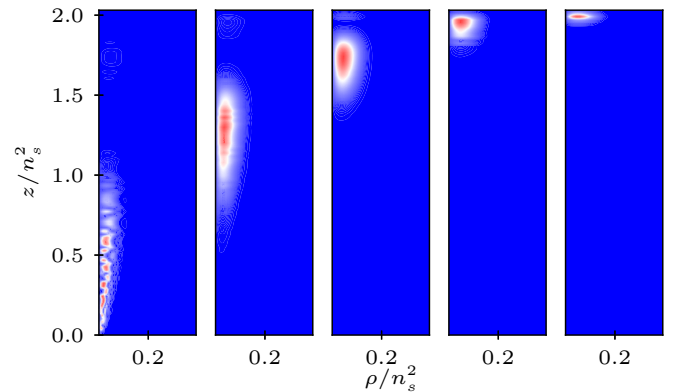


FIG. 2. Topological localization of a Rydberg electron. Probability densities of an eigenstate of (3) corresponding to one of the edge states identified with the help of (2). The densities are plotted in the laboratory frame and in the cylindrical coordinate for different moments of time, i.e., $\omega t/s = 7\pi/4 + j\pi/4$ where integer $j$ goes from 0 to 4 from left to right panels, respectively. The presented edge state reveals the wavepacket evolving on the elongated Kepler orbit with the period $s2\pi/\omega$ and its localization is protected by topology. The sequence of the panels illustrates time evolution of the wavepacket during one half of the period. During the other half, the time evolution can be illustrated by the same panels but ordered from right to left. The parameters are the same as in Fig. 1(b). Quantities are in atomic units.

the electron is represented by a wavepacket that periodically propagates on the elongated ellipse and does not spread because its localization is protected by topology. This behavior is resistant to a perturbation of the effective Hamiltonian, unless the perturbation is so strong that the gap between the bands is closed [20].

In Ref. [10] nonspreading wavepackets of a Rydberg electron are described. However, their formation has nothing to do with topological protection. They are related to the trapping of a Rydberg electron in a single well of an effective potential that is created by the 1 : 1 resonant driving of the H atom. The mechanism of the formation of the localized states considered in this Letter is completely different. The localized states are edge states with localization length $\xi \propto 1/\ln(J'/J)$, where $J$ and $J'$ are tunneling rates of an electron through the higher and lower barriers, respectively, of the effective potential in (2) [23]. The localization length $\xi$ can be much larger than the size of a single well of the effective potential in (2). Topological protection means that if we change the parameters of the effective model (2), $\xi$ can change but the localization phenomenon itself will not be broken, provided that the energy gap is not closed.

*Topological molecules.* Attractive interactions between charge particles allow atoms to form molecules. It is also possible to create bound states of atoms if the interaction potential between them changes in a disordered way as a function of their relative distances. Then, they can form the so-called Anderson molecules that are created due to destructive interference and the resulting Anderson localization [8,30,31]. Here we show that it is possible to realize bound states of atoms which have a topological origin. We will see that the description of two atoms with the interaction strength modulated in time can be reduced to the effective Hamiltonian where we can identify a *center-of-mass* degree of freedom described by the free particlelike Hamiltonian and the *relative position* degree of freedom described by the Hamiltonian (2). The edge states of the Hamiltonian (2) will correspond to the molecular bound states protected by topology.

Let us consider two atoms which are moving in the one-dimensional (1D) infinite well potential. For simplicity, we assume that they are the same atomic species but in different hyperfine states. The infinite well potential in one dimension can be created experimentally if, in a three-dimensional trap, with strong transverse confinement, two barriers are implemented that limit the motion of the atoms along the longitudinal direction [32]. At low kinetic energies, the interaction between atoms can be modeled by means of the contact Dirac delta potential with the strength $g$ proportional to the $s$-wave scattering length of the atoms. We assume that $g(t)$ is modulated periodically in time by means of Feshbach resonance [33] or confinement-induced resonance [34] so that the Hamiltonian of the system reads

$$H = \frac{p_1^2 + p_2^2}{2} + g(t)\delta(x_1 - x_2), \qquad (4)$$

where $g(t) = F_1 \cos(\omega t) + F_2 \cos(2\omega t) + \lambda f(t)$. We have used $\pi^2 \hbar^2 / mR^2$ and $R/\pi$ as units of energy and length, respectively, where $R$ is the size of the potential well and $m$ is the mass of the atoms. For simplicity, we have used the same notation for the parameters of $g(t)$ as in the case of a

H atom [cf. (1)], but now $F_j$ and $\lambda$ are quantities proportional to the $s$-wave scattering length of the atoms. As previously, $f(t) = f(t + s2\pi/\omega) = \sum_{k \neq 0} f_k e^{ik\omega t/s}$. In the units that we use, the motion of the atoms is limited between 0 and $\pi$ due to the presence of the potential walls. Thus, the wavefunction vanishes if $x_1$ or $x_2$ equals 0 or $\pi$.

To describe the system, it is sufficient to restrict to the subspace of symmetric combinations of the eigenstates of the noninteracting atoms, i.e., $\Phi_{n_1,n_2} = [\phi_{n_1,n_2} + \phi_{n_2,n_1}]/\sqrt{2}$ for $n_1 > n_2$ and $\Phi_{n_1,n_1} = \phi_{n_1,n_1}$, where $\phi_{n_1,n_2}(x_1, x_2) = 2\sin(n_1 x_1)\sin(n_2 x_2)/\pi$, because there is no interaction between the atoms in the antisymmetric subspace [20]. We are interested in the resonant behavior of the system where $n_1 \approx \omega/2s$ and $n_2 \approx \omega/2s$. Switching to the moving frame by means of the unitary transformation $e^{i(\hat{n}_1 + \hat{n}_2)\omega t/2s}$ and averaging the resulting Hamiltonian over time, we arrive at the matrix of the quantum effective Hamiltonian $\hat{H}_{\text{eff}}$ that consists of independent blocks labeled with different values of $n_{\text{c.m.}} = n_1 - n_2$. That is, in a given $n_{\text{c.m.}}$ block the matrix elements of the $\hat{H}_{\text{eff}}$ read [20]

$$\begin{aligned} \langle n'|\hat{H}_{\text{eff}}|n\rangle = &\, n^2 \delta_{n',n} + \frac{F_1}{2\pi}(\delta_{n',n+s} + \delta_{n',n-s}) \\ &+ \frac{F_2}{2\pi}(\delta_{n',n+2s} + \delta_{n',n-2s}) + \frac{\lambda}{\pi}f_{n'-n} \\ &+ \frac{n_{\text{c.m.}}^2}{4}\delta_{n',n}, \end{aligned} \qquad (5)$$

where $n = (n_1 + n_2)/2 - \omega/2s$. The position operators conjugate to the quantum numbers $n_{\text{c.m.}}$ and $n$ are $x_{\text{c.m.}} = (x_1 - x_2)/2$ and $x = x_1 + x_2$, respectively. This effective description is valid in the subspace $|n| \ll \omega/2s$.

Apart from the last term, the matrix (5) is identical to the matrix of the quantized version of the classical effective Hamiltonian (2) calculated in the plane-wave basis, $e^{in\Theta}/\sqrt{2\pi}$, if the effective mass $m_{\text{eff}} = 1/2$, $V_j = F_j/\pi$, and $V_b = \sum_{k \neq 0} f_k e^{ik\Theta}/\pi$. Thus, the two-atom system behaves like a two-particle system whose center-of-mass position $x_{\text{c.m.}}$ (conjugate to the momentum quantum number $n_{\text{c.m.}}$) moves like a free particle [cf. the term $n_{\text{c.m.}}^2/4$ in (5)] while the relative position $x$ can possess topologically protected edge states corresponding to the bound states of the particles. Particles prepared in an edge state form a topological molecule in which their relative position $x$ is described by a localized state that is protected by topology.

Our secular approximation approach allows us to identify parameters suitable for the realization of a topological molecule, but we are also able to describe the system exactly by numerical diagonalization of the Floquet Hamiltonian $H_F = H - i\partial_t$ where $H$ is given in (4) [10,20,35]. The eigenstates of $H_F$ are called Floquet states which evolve with the same period as the period of $g(t)$ and the corresponding eigenvalues are quasienergies of the system. The eigenstates of the effective Hamiltonian (5) also evolve periodically in time when we return to the laboratory frame, and they constitute a very good approximation of the exact Floquet eigenstates of $H_F$.

In Fig. 3(a) we show the exact Floquet states, in the moving frame, that correspond to the edge states described above.
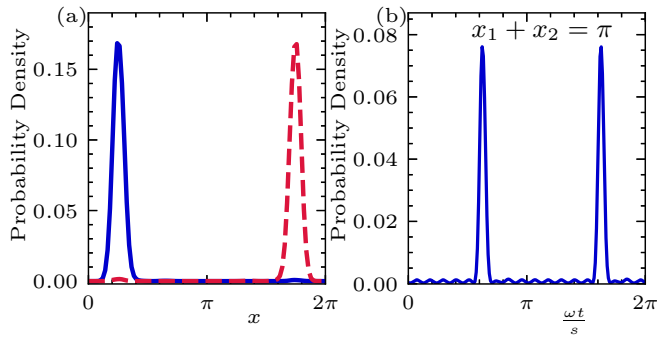
FIG. 3. Topological molecules. Panel (a) shows probability densities of two edge states in the moving frame. The densities are localized around the certain position $x$, indicating that two atoms form bound states. Panel (b) presents signatures of the formation of the topological molecule in the laboratory frame. If the atoms are prepared in, e.g., the edge state drawn with the blue line in (a), the probability density for the measurement of the atoms at $x_1 + x_2 = \pi$ reveals a periodic appearance of the localized edge state. The results are obtained within the exact diagonalization of the Floquet Hamiltonian, but they are indistinguishable from the densities obtained with the help of the effective Hamiltonian (5). The parameters of the system are the following: $F_1/F_2 = 2$ with $F_2 = 10$, $\omega = 10^5$, $\lambda = 35$ and the Fourier components of $f(t)$ are $f_k = e^{ik\epsilon}\cos(k\pi/21)\text{sinc}^2(k\pi/14)$ with $\epsilon = 10^{-4}$ for $|k| \leqslant 40$ and $f_k = 0$ for greater $|k|$. Unit are specified following Eq. (4).

The probability densities describing the position $x$, which is conjugate to the quantum number $n$, perfectly match the edge state probability densities obtained with the help of the effective Hamiltonian (5). It confirms that the atoms can form topologically protected bound states. When the system is observed in the laboratory frame, the signatures of the formation of the topological molecule are illustrated in Fig. 3(b). That is, the probability density for the atoms to be observed at $x_1 + x_2 = \pi$ reveals a periodic appearance of the localized edge state.

*Conclusions.* We have shown that topology is capable of protecting the states of the atomic constituents. A Rydberg electron can be represented by a localized wavepacket moving along a classical orbit, and such a localization is protected by topology. A similar mechanism is responsible for the formation of topological molecules—bound states of particles protected by topology.

We have considered the localization of a Rydberg electron on a Kepler orbit aligned along the static electric field direction. However, one may expect that the topological localization can also be observed on Kepler orbits with different shapes. That is, the static electric field allows one to control the shape of a stable Kepler ellipse [21], and similar microwave fields as we have used here should lead to the topological localization of the electron on the ellipse. The experimental setup for realization of the phenomenon we predict can be very similar to the procedure used in Refs. [13–16] where nonspreading Rydberg wavepackets were demonstrated.

Ultracold atoms in a quasi-1D squared well potential [32] seem to be a suitable system for the realization of topological molecules. Two localized clouds of atoms can be pushed to motion, and if it is done at proper phase of the time-periodic modulation of the strength of interactions between atoms, the clouds will be locked to a localized edge state of an effective topological model that describes the system [20]. Modulation of the interaction strength can be done by means of the Feshbach resonance [33] or the confinement-induced resonance in quasi-1D potentials [34,36].

[1] C. Nayak, S. H. Simon, A. Stern, M. Freedman, and S. Das Sarma, Rev. Mod. Phys. **80**, 1083 (2008).

[2] M. Z. Hasan and C. L. Kane, Rev. Mod. Phys. **82**, 3045 (2010).

[3] L. Guo, M. Marthaler, and G. Schön, Phys. Rev. Lett. **111**, 205303 (2013).

[4] K. Sacha, Phys. Rev. A **91**, 033617 (2015).

[5] K. Sacha, Sci. Rep. **5**, 10787 (2015).

[6] K. Sacha and J. Zakrzewski, Rep. Prog. Phys. **81**, 016401 (2018).

[7] L. Guo and P. Liang, New J. Phys. **22**, 075003 (2020).

[8] K. Sacha, *Time Crystals* (Springer International Publishing, Cham, 2020).

[9] L. Guo, *Phase Space Crystals* (IOP Publishing, Philadelphia, PA, 2021).

[10] A. Buchleitner, D. Delande, and J. Zakrzewski, Phys. Rep. **368**, 409 (2002).

[11] D. Delande and A. Buchleitner, in *Advances In Atomic, Molecular, and Optical Physics*, edited by B. Bederson and H. Walther (Academic, New York, 1994), Vol. 34, pp. 85–123.

[12] I. Bialynicki-Birula, M. Kaliński, and J. H. Eberly, Phys. Rev. Lett. **73**, 1777 (1994).

[13] H. Maeda and T. F. Gallagher, Phys. Rev. Lett. **92**, 133004 (2004).

[14] H. Maeda and T. F. Gallagher, Phys. Rev. A **75**, 033410 (2007).

[15] H. Maeda, J. H. Gurian, and T. F. Gallagher, Phys. Rev. Lett. **102**, 103001 (2009).

[16] B. Wyker, S. Ye, F. B. Dunning, S. Yoshida, C. O. Reinhold, and J. Burgdörfer, Phys. Rev. Lett. **108**, 043001 (2012).

[17] K. Giergiel and K. Sacha, Phys. Rev. A **95**, 063402 (2017).

[18] M. T. Eiles, A. Eisfeld, and J. M. Rost, arXiv:2111.10345.

[19] A. Lichtenberg and M. Lieberman, *Regular and Chaotic Dynamics*, Applied Mathematical Sciences (Springer-Verlag, Berlin, 1992).

[20] See Supplemental Material at http://link.aps.org/supplemental/10.1103/PhysRevA.106.L031301 for the details of the derivation of the classical and quantum effective Hamiltonians and the discussion of robustness of the realization of the effective models.

[21] K. Sacha, J. Zakrzewski, and D. Delande, Eur. Phys. J. D **1**, 231 (1998).

[22] W. P. Su, J. R. Schrieffer, and A. J. Heeger, Phys. Rev. Lett. **42**, 1698 (1979).

[23] J. Asbóth, L. Oroszlány, and A. Pályi, *A Short Course on Topological Insulators: Band Structure and Edge States in One and Two Dimensions*, Lecture Notes in Physics (Springer International Publishing, New York, 2016).

[24] N. R. Cooper, J. Dalibard, and I. B. Spielman, Rev. Mod. Phys. **91**, 015005 (2019).

[25] M. Atala, M. Aidelsburger, J. T. Barreiro, D. Abanin, T. Kitagawa, E. Demler, and I. Bloch, Nat. Phys. **9**, 795 (2013).

[26] E. J. Meier, F. A. An, and B. Gadway, Nat. Commun. **7**, 13986 (2016).

[27] P. St-Jean, V. Goblot, E. Galopin, A. Lemaître, T. Ozawa, L. Le Gratiet, I. Sagnes, J. Bloch, and A. Amo, Nat. Photonics **11**, 651 (2017).

[28] K. Giergiel, A. Dauphin, M. Lewenstein, J. Zakrzewski, and K. Sacha, New J. Phys. **21**, 052003 (2019).

[29] The chosen Fourier components $f_k$ allow one to realize a bar-

rier in the effective model (2). This barrier can be realized in many different ways (see [20]). The small parameter $\epsilon$ breaks the reflection symmetry of the potential in the effective SSH model; if such a symmetry was present, the edge states would be superpositions of the localized wavepackets presented in Fig. 1(b).

[30] K. Giergiel, A. Miroszewski, and K. Sacha, Phys. Rev. Lett. **120**, 140401 (2018).

[31] P. Matus, K. Giergiel, and K. Sacha, Phys. Rev. A **103**, 023320 (2021).

[32] A. L. Gaunt, T. F. Schmidutz, I. Gotlibovych, R. P. Smith, and Z. Hadzibabic, Phys. Rev. Lett. **110**, 200406 (2013).

[33] C. Chin, R. Grimm, P. Julienne, and E. Tiesinga, Rev. Mod. Phys. **82**, 1225 (2010).

[34] M. Olshanii, Phys. Rev. Lett. **81**, 938 (1998).

[35] J. H. Shirley, Phys. Rev. **138**, B979 (1965).

[36] E. Haller, M. J. Mark, R. Hart, J. G. Danzl, L. Reichsöllner, V. Melezhik, P. Schmelcher, and H.-C. Nägerl, Phys. Rev. Lett. **104**, 153203 (2010).

[37] S. Balay, S. Abhyankar, M. F. Adams, J. Brown, P. Brune, K. Buschelman, L. Dalcin, A. Dener, V. Eijkhout, W. D. Gropp *et al.*, Technical Report No. ANL-95/11–Revision 3.12, Argonne National Laboratory, 2019, https://www.mcs.anl.gov/petsc.

[38] S. Balay, W. D. Gropp, L. C. McInnes, and B. F. Smith, in *Modern Software Tools in Scientific Computing*, edited by E. Arge, A. M. Bruaset, and H. P. Langtangen (Birkhäuser, Basel, Switzerland, 1997), pp. 163–202.

[39] V. Hernandez, J. E. Roman, and V. Vidal, ACM Trans. Math. Softw. **31**, 351 (2005).